Cell Stem Cell
Article

miR-130b Promotes CD133$^+$ Liver Tumor-Initiating Cell Growth and Self-Renewal via Tumor Protein 53-Induced Nuclear Protein 1

Stephanie Ma,[1,5,*] Kwan Ho Tang,[1] Yuen Piu Chan,[1] Terence K. Lee,[1,5] Pak Shing Kwan,[2] Antonia Castilho,[1,5] Irene Ng,[1,5] Kwan Man,[3,5] Nathalie Wong,[6] Ka-Fai To,[6] Bo-Jian Zheng,[4] Paul B.S. Lai,[7] Chung Mau Lo,[3] Kwok Wah Chan,[1,*] and Xin-Yuan Guan[2,5,*]
[1]Department of Pathology
[2]Department of Clinical Oncology
[3]Department of Surgery
[4]Department of Microbiology
[5]State Key Laboratory for Liver Research
Li Ka Shing Faculty of Medicine, Queen Mary Hospital, The University of Hong Kong, Hong Kong
[6]Department of Anatomical and Cellular Pathology
[7]Department of Surgery
Prince of Wales Hospital, The Chinese University of Hong Kong, Hong Kong
*Correspondence: stefma@hkucc.hku.hk (S.M.), kwchan@pathology.hku.hk (K.W.C.), xyguan@hkucc.hku.hk (X.-Y.G.)
DOI 10.1016/j.stem.2010.11.010

SUMMARY

A novel paradigm in tumor biology suggests that cancer growth is driven by stem-like cells within a tumor, called tumor-initiating cells (TICs) or cancer stem cells (CSCs). Here we describe the identification and characterization of such cells from hepatocellular carcinoma (HCC) using the marker CD133. CD133 accounts for approximately 1.3%–13.6% of the cells in the bulk tumor of human primary HCC samples. When compared with their CD133$^-$ counterparts, CD133$^+$ cells not only possess the preferential ability to form undifferentiated tumor spheroids in vitro but also express an enhanced level of stem cell-associated genes, have a greater ability to form tumors when implanted orthotopically in immunodeficient mice, and can be serially passaged into secondary animal recipients. Xenografts resemble the original human tumor and maintain a similar percentage of tumorigenic CD133$^+$ cells. Quantitative PCR analysis of 41 separate HCC tissue specimens with follow-up data found that CD133$^+$ tumor cells were frequently detected at low quantities in HCC, and their presence was also associated with worse overall survival and higher recurrence rates. Subsequent differential microRNA expression profiling of CD133$^+$ and CD133$^-$ cells from human HCC clinical specimens and cell lines identified an overexpression of miR-130b in CD133$^+$ TICs. Functional studies on miR-130b lentiviral-transduced CD133$^-$ cells demonstrated superior resistance to chemotherapeutic agents, enhanced tumorigenicity in vivo, and a greater potential for self renewal. Conversely, antagonizing miR-130b in CD133$^+$ TICs yielded an opposing effect. The increased miR-130b paralleled the reduced TP53INP1, a known miR-130b target. Silencing TP53INP1 in CD133$^-$ cells enhanced both self renewal and tumorigenicity in vivo. Collectively, miR-130b regulates CD133$^+$ liver TICs, in part, via silencing TP53INP1.

INTRODUCTION

Human epithelial cell-derived cancers are highly heterogeneous in their morphologies, clinical behaviors, and molecular profiles. The tumor-initiating cell (TIC) or cancer stem cell (CSC) concept suggests that tumors are organized in a hierarchy of mixed tumor cells and that sitting at the apex is a subset of cancer cells that are biologically distinct from the others and bear stem cell-like features, which are indispensable for a tumor. These TICs possess both self renewal and differentiation capabilities and are believed to give rise to tumor heterogeneity (Visvader and Lindeman, 2008; Jordan et al., 2006; Pardal et al., 2003). Thus, TIC eradication may be critical to achieving stable remission of, and even curing, aggressive malignancies. To date, the perpetuations of many cancer types, including leukemia, breast cancer, brain cancer, prostate cancer, colon cancer, and hepatocellular carcinoma (HCC) have been suggested to stem from TICs.

HCC ranks as the fifth most prevalent cancer worldwide, affecting 1 million individuals annually (Jemal et al., 2009). Surgical resection and liver transplantation are available for early-stage HCC, but because most patients are diagnosed at advanced stages, only 25% of patients with this cancer are amenable to surgery. Chemotherapy is one of the main treatments given to the remaining patients with inoperable HCC and is also administered as a pre-/postsurgical adjuvant therapy, yet the overall response rate to this treatment is low due to the highly chemotherapy-resistant nature of the disease (Aravalli et al., 2008). Therefore, understanding the mechanism underlying hepatocarcinogenesis is essential for managing HCC.

Recently, we have identified a TIC population from HCC cells and xenograft tumors that is marked by a CD133 surface

phenotype and bears features that include the abilities to self renew; differentiate into non-hepatocyte-like, angiomyogenic-like lineages; initiate tumors in vivo and resist standard chemotherapy via the Akt/PKB and Bcl-2 pathways (Ma et al., 2007, 2008). Our findings also correspond with reports by other research groups (Suetsugu et al., 2006; Yin et al., 2007; Zhu et al., 2010; Song et al., 2008), thus demonstrating the prominence of CD133 as a marker for TICs in HCC cell lines.

MicroRNAs (miRNAs) are an abundant class of small, noncoding RNAs that negatively regulate gene expression at the post-transcriptional level by inhibiting ribosome function, decapping the 5′cap structure, deadenylating the poly(A) tail, and degrading the target mRNA (He and Hannon, 2004; Filipowicz et al., 2008). miRNAs can regulate and control a variety of biological processes including developmental timing, signal transduction, stem cell self renewal, and differentiation (Gangaraju and Lin, 2009; Croce and Calin, 2005; Inui et al., 2010). One of the best-studied miRNAs, let-7 in *C. elegans*, was initially identified in mutants with defects in developmental timing (Reinhart et al., 2000). The loss of dicer1, an important endonuclease for the synthesis of mature miRNAs, also induces embryonic lethality and depletion of stem cells (Bernstein et al., 2003; Hatfield et al., 2005). In addition, tissue-specific deletion of dicer affects the self renewal of embryonic stem cells, the development of B lymphocyte lineage cells, and tissue morphogenesis (Chen et al., 2008; Davis et al., 2008; Koralov et al., 2008). The deletion of DGCR8, another key enzyme for miRNA processing, alters the silencing of self-renewal genes in embryonic stem cells (Wang et al., 2007). Moreover, a distinct miRNA subset is specifically expressed in pluripotent embryonic stem cells but not in adult tissues (Suh et al., 2004).

In addition to regulating cell-fate decisions, some miRNAs can also function as tumor promoters or suppressors, regulating the maintenance and progression of cancers and TICs (DeSano and Xu, 2009; Esquela-Kerscher and Slack, 2006). The expression of let-7 prevents tumor sphere formation in breast cancer cell lines and inhibits tumorigenicity in an in vivo xenograft tumor assay (Yu et al., 2007). Elevated miR-181 family members were identified as critical players in regulating EpCAM+ hepatic TICs (Ji et al., 2009), and the downregulation of miR-200 family miRNAs suggests that normal stem cells and breast cancer stem cells share common molecular mechanisms that regulate stem cell functions, such as self renewal, proliferation, and the epithelial-mesenchymal transition (Shimono et al., 2009). Finally, miRNA expression profiles have been correlated with the tumor stage, progression, and prognosis of cancer patients (Jiang et al., 2008; Ura et al., 2009; Calin et al., 2005; Iorio et al., 2005). These findings demonstrate that miRNAs are critical regulators of self renewal, differentiation, and carcinogenesis.

To date, CD133 has only been used to identify liver TICs in cell-line-based models. The characterization of this specific population of cells is also very limited. In this study, we first validated CD133 as a marker for liver TICs in freshly resected HCC clinical specimens and identified a prognostic role of CD133 in HCC. Subsequently, we elucidated the underlying molecular mechanism by which this specific population of cells mediates tumor formation and growth by a systematic comparison of the miRNA profiles in CD133+ liver TICs and their differentiated progeny. Our findings suggest that HCC maintenance and growth is dictated, at least in part, by a CD133+-expressing subpopulation and that miR-130b regulates the growth and self renewal of CD133+ liver TICs via the direct targeting of TP53INP1.

RESULTS

Identification of CD133+ as Liver TICs in Human HCC Clinical Specimens

Previous work from our laboratory identified a TIC population marked by the CD133 surface phenotype in HCC xenograft tumors and cell lines. CD133+ cells were found capable of extensive proliferation, exhibited an increased potential to self renew and differentiate, expressed stem cell-associated markers and were maintained at a low frequency in the bulk of the tumor mass (Ma et al., 2007). CD133+ cells also contribute to HCC chemoresistance through Akt/PKB and Bcl-2 pathway activations (Ma et al., 2008). The identification and characterization of a CD133+ TIC population in HCC xenograft tumors and cell lines suggested that CD133 may also represent a TIC marker in primary human HCC specimens. Therefore, as a first step, we examined the expression of CD133 in fresh tissue samples derived from patients with HCC using both flow cytometry and immunohistochemistry (IHC). In total, 35 individual patients were analyzed. Flow cytometry demonstrated the presence of a rare CD133 population in HCC specimens, with expression ranging from 1.3% to 13.6% (Figure 1A). A potential contamination of the CD133+ cell population by hematopoietic and endothelial progenitors was excluded by flow cytometry using CD45 and CD31, respectively. CD133+ cells were negative for the pan-hematopoietic marker CD45, and less than 1.3% of the CD133+ subpopulation was putative CD31+ endothelial progenitors (Figure 2A). Consistently, histological analysis revealed that similar percentages of CD133+ cells were localized in the bulk tumor (Figure 1B). All HCC samples reproducibly demonstrated the presence of only a rare CD133+ population, while, in contrast, CD133 expression in nontumor (NT) liver tissues was almost nonexistent (Figures 1A and 1B). Due to the short follow-up period after the fresh clinical specimens were collected, the association between CD133 expression and disease-free survival or overall survival could not be calculated. However, quantitative real-time PCR (qPCR) analysis of 41 HCC tissue specimens that we had collected earlier and for which we have follow-up data showed that increased CD133 expression in HCC not only correlated with advanced disease stage but also was associated with higher recurrence rates and worse overall survival. Increased CD133 expression in HCC was more associated with higher tumor stages (T stages III or IV) than with lower tumor stages (T stages I or II) (χ^2 test, $p = 0.008$; Figure 1C and Table S1). Furthermore, an association study showed the CD133 ΔCt value to be inversely correlated with tumor stage in these 41 HCC patients ($n = 38$, Pearson correlation, $r = -0.428$, χ^2 test, $p = 0.007$). In a Kaplan-Meier survival analysis, patients with CD133+ primary tumors displayed worse disease-free survival (estimated mean = 13.75 months) when compared to those patients with $CD133^{-/low}$ primary tumors (estimated mean = 61.49 months) (log-rank test, $p = 0.001$; Figure 1D). In addition, CD133 expression was also associated with long-term overall survival. Patients with CD133+ primary tumors had a mean overall survival of 27.11 months, as compared with 78.51 months for

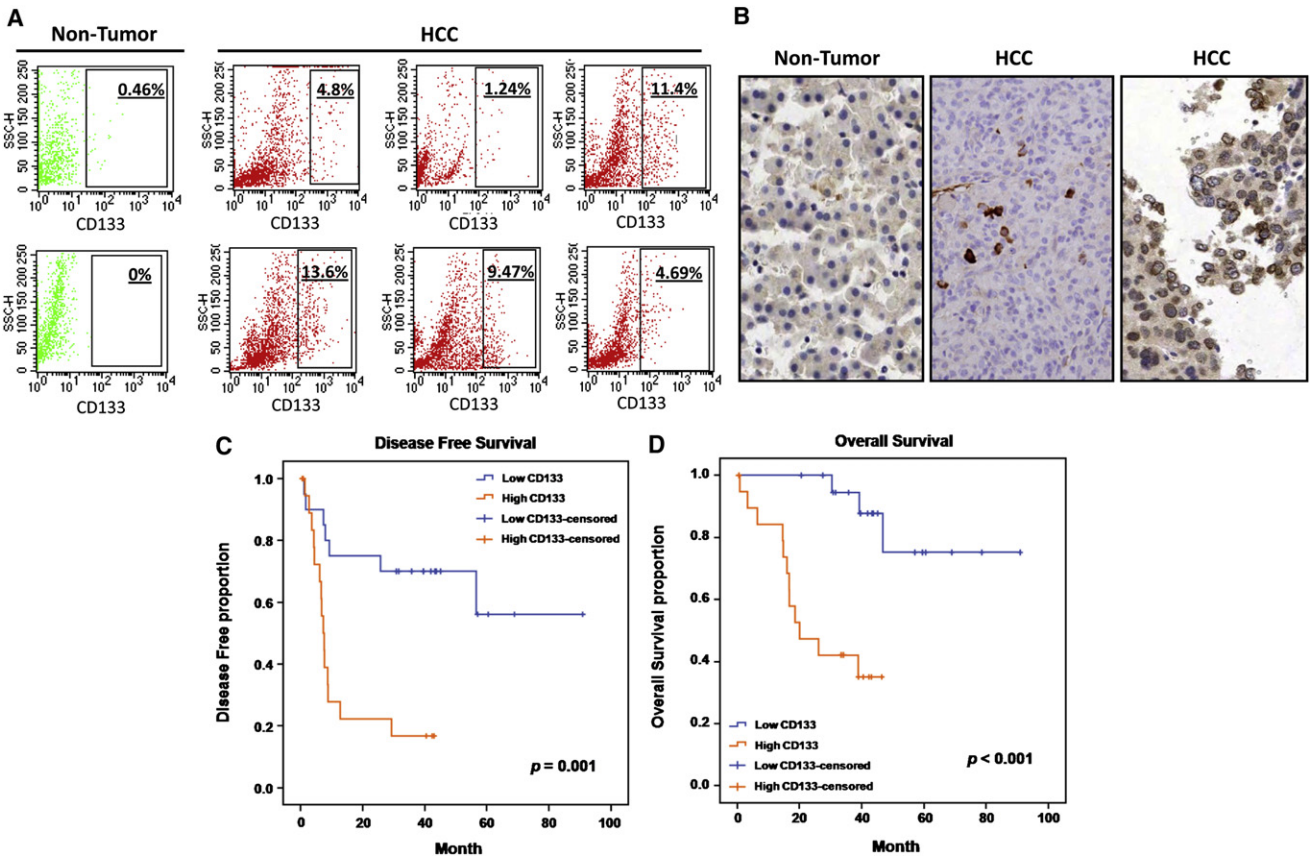

Figure 1. CD133 Expression in HCC Clinical Specimens Is Associated with Advanced Tumor Stage and Poor Prognosis

(A–D) Single cells digested from freshly resected NT or HCC tissue samples or their corresponding paraffin-embedded formalin-fixed tissue sections were stained for CD133 and analyzed by either (A) flow cytometry or (B) IHC. Tissue sections were counterstained with H&E. IHC images were taken at 200× magnification. In total, 35 individual patients were analyzed. qPCR analysis for CD133 expression in 41 HCC tissue specimens found that elevated CD133 expression was associated with (C) higher recurrence rates (log-rank test, $p = 0.001$) and (D) worse overall survival (log-rank test, $p < 0.001$). The disease-free survival and overall survival rates significantly decreased in HCC patients with high CD133 expression (orange line; $n = 20$) compared with HCC patients with low CD133 expression (blue line; $n = 20$). See also Tables S1 and S2.

patients with $CD133^{-/low}$ primary tumors (log-rank test, $p < 0.001$). Univariate Cox regression analysis also identified that the tumor stage was significantly associated with disease-free survival and that the CD133 expression was correlated with both disease-free and overall survival (Table S2). CD133 expression was, however, not significantly associated with age, gender, α-fetoprotein (AFP) levels, or tumor size (Table S1).

Next, we evaluated the tumorigenic potential and stem cell-like properties of isolated $CD133^+$ TICs from freshly resected HCC. Preliminary data demonstrated that following tumor dissociation into single cells, cells must be at least 70% viable in order for experiments like in vivo tumorigenicity assays and in vitro spheroid formation assays to be successful. Among the 83 matched NT and HCC specimens collected, cells isolated from only one-fourth ($n = 21$) of the tumor specimens showed >70% cell viability. Thus, only these 21 samples were used for further downstream studies, following initial screening for CD133 expression by flow cytometry ($n = 35$). Following the removal of dead cells, $CD133^+$ TICs were isolated by magnetic bead sorting, which resulted in a considerable enrichment of $CD133^+$ cells (purity 82%–92%) and, more importantly, a higher negative selection (purity >98%) of $CD133^-$ cells. Again, potential contamination of the $CD133^+$ cell population by hematopoietic and endothelial progenitors was excluded by flow cytometry using CD45 and CD31, respectively (Figure 2A; bottom).

Following sorting, we investigated the ability of tumor-derived $CD133^+$ and $CD133^-$ cells to orthotopically engraft and give rise to tumors in SCID/Beige mice. As many as 5×10^5 patient-derived $CD133^-$ HCC cells resuspended in Matrigel were needed to initiate occasional tumor formation, while, in contrast, as few as 2×10^4 $CD133^+$ cells resuspended in Matrigel generated visible tumors 8 weeks postinjection (Figure 2B and Table S3; data representative of eight tumors tested). These data indicate that cells capable of initiating HCC are highly enriched within a $CD133^+$ cell population. Additionally, histological analysis revealed that tumor xenografts derived from $CD133^+$ cells consistently reproduced the primary tumor at the histological level (data not shown). To investigate whether $CD133^+$ HCC cells display long-term tumorigenic potential, we evaluated their ability to generate tumors in serial transplantations. Sorted $CD133^+$ and $CD133^-$ cells from primary tumor xenografts were transplanted into secondary mouse recipients. Only $CD133^+$

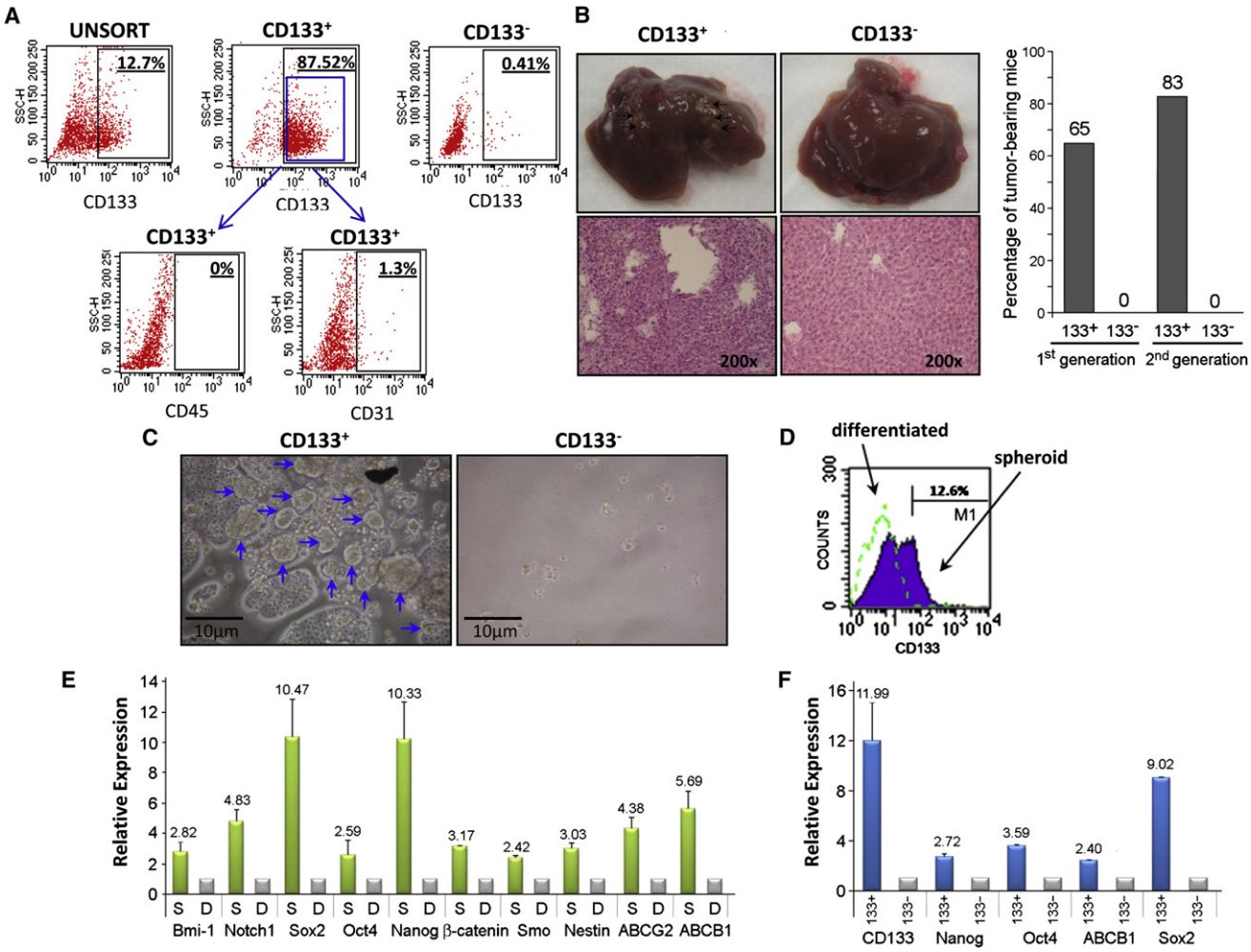

Figure 2. Tumorigenic and Stem Cell-like Potential of CD133+ Cells in Patient-Derived HCC Samples

(A) A flow cytometry dot plot shows the distribution of CD133+ cells in unsorted and sorted freshly resected human HCC specimens. Purity for the positive fraction ranged from 82%–92%, while the negative fraction achieved greater than 98% purity. Flow cytometry for CD31 and CD45 was performed to detect potential contamination of isolated cells with endothelial or hematopoietic progenitors. Staining revealed no or very low expression of these cell types in the CD133+ TIC population.

(B) CD133+ TICs isolated from freshly isolated tumors, but not CD133− cells, were capable of inducing tumor formation when orthotopically implanted into the liver of SCID/Beige mice. See also Table S3. H&E staining of tumors injected with CD133+ TICs revealed malignant cells. Serial transplantation of xenografted tumors in secondary animal recipients showed enhanced engraftment ability, as demonstrated by the increased number of tumor-bearing mice.

(C) CD133+ TICs were able to generate an increased number of primary and serially passaged spheroids as compared with CD133− cells in freshly isolated tumors.

(D–F) A flow cytometry histogram analysis shows the enrichment of CD133 expression in mechanically dissociated CD133+ spheroids (purple; "spheroid") as compared to the differentiated adherent counterpart (dotted green; "differentiated"). qPCR analysis was performed for stem cell-associated and multiple-drug-resistant transporter genes in (E) mechanically dissociated cancer spheroids ("S") versus primary adherent HCC cells ("D") and (F) CD133+ TICs versus CD133− cells isolated from freshly resected tumors. Differentiated adherent cells and CD133− were defined as 1 (calibrator), and the relative expression of each gene was expressed as the fold difference over this baseline. β-actin was used as an internal control.

tumor cells successfully engrafted. Secondary tumors grew better, as evident by the number of tumor-bearing mice (83% in secondary xenografts versus 65% in primary xenografts), and they grew more rapidly than those tumors in the primary xenografts (Figure 2B). Tumor morphologies were indistinguishable from either tumors generated from primary animal recipients or original tumors. Thus, the CD133+ cell population resident in the HCC tumor mass could generate serial xenografts, suggesting an in vivo self-renewing capacity.

Next, we examined the ability of CD133+ TICs and CD133− cells to grow as spheroids in nonadherent, serum-free, growth factor-supplemented conditions that favor the proliferation of undifferentiated cells. Within 3 weeks of culture, we obtained HCC spheres of growing undifferentiated CD133+ cells. CD133− tumor cells invariably died in such serum-free conditions (Figure 2C; data representative of seven tumors tested). More importantly, single cells obtained from these CD133+ dissociated spheres could be clonally expanded in subsequent

serial propagations, showing virtually unlimited growth potential. When CD133+ cells were grown as HCC spheres, these cells remained CD133+. To determine the differentiation potential of these CD133+ cells, tumor spheres were cultivated without EGF and FGF2 in the presence of 10% serum. After several days of culture, the spheres differentiated, attached onto the flasks, and grew as adherent cells. As compared with undifferentiated spheres, adherent counterparts expressed less CD133 expression following induced in vitro differentiation (Figure 2D; data representative of seven tumors tested). The ability of CD133+ cells to form spheres and be serially propagated suggests an in vitro self-renewing capacity. Similarly, the proportions of stem cell-associated genes, including *Bmi-1*, *Notch 1*, *Sox2*, *Oct-4*, *nanog*, β-*catenin*, *Smo*, and *nestin*, and multidrug resistance transporters *ABCG2* and *ABCB1* were reduced following in vitro differentiation of CD133+ TIC spheres (Figure 2E; data representative of three tumors tested). In addition, patient-derived CD133+ TICs also expressed an enhanced level of stem cell-associated genes, including *nanog*, *Oct-4*, *ABCB1*, and *Sox2*, when compared with their CD133− tumor counterparts (Figure 2F; data representative of three tumors tested). Collectively, these data demonstrate the existence of a TIC population in HCC marked by a CD133 surface phenotype and bearing cancer and stem cell-like features including the ability to self renew, differentiate, and initiate tumors in vivo.

miRNA Profiling of CD133+ TICs and CD133− Cell Counterparts

Following the identification of CD133+ liver TICs, we furthered our study to characterize the underlying mechanism that drives this population of cells and their role in tumor progression. miRNAs are recognized as important regulators of posttranscriptional gene expression, regulating both cellular differentiation and embryonic stem cell development as well as tumor progression. In light of this, we postulated whether differences in miRNA expression might distinguish CD133+ TICs from their more differentiated progeny. We profiled isolated CD133+ TICs and CD133− cells from freshly resected tumors from HCC patients (n = 5) and HCC cell lines (n = 2; Huh7 and PLC8024) using a SYBR Green-based qPCR miRNA array containing 95 well-characterized human miRNAs known to be involved specifically in stem cell self renewal and differentiation. miRNAs that displayed >2-fold changes in HCC patients and cell lines were tabulated. Altogether, 5 upregulated and 24 downregulated miRNAs were found among the clinical HCC specimens. In parallel, four reproducibly upregulated and nine downregulated miRNAs were identified across all HCC cell lines. We reasoned that relevant miRNAs should commonly appear in both primary tumors and HCC cell lines. Therefore, we combined the two different data sets in a Venn diagram and observed a total of eight expression-altered miRNAs common to all cells: two upregulated (miR-130b and miR-369-5p) and six downregulated (let-7a, miR-30c, miR-33, miR-153, miR-1, and miR-10b) (Figure 3A). To validate our profiling findings, we performed a second round of qPCR using the more precise TaqMan primers on selected commonly deregulated miRNAs sorted by CD133 from HCC cells PLC8024 and Huh7, as well as a on a series of liver cell lines with differing CD133 expression levels (data not shown). Preferential deregulation of the miRNAs was indeed verified, whereas, in parallel assays, two control miRNAs (miR-24 and miR-92) were found to be unchanged in expression (data not shown). However, only the expression of miR-130b could be closely correlated with CD133 expression in the examined series of liver cell lines (Figure 3B). Liver cell lines with low CD133 expression had relatively lower levels of miR-130b (HepG2, H2P, H2M), while, in contrast, liver cell lines with high CD133 levels expressed relatively higher levels of miR-130b (PLC8024, Huh7, Hep3B) (Figures 3B and S1). In view of this, together with the high fold-change difference in CD133+ TICs, we further focused our studies on miR-130b.

miR-130b Is Preferentially Expressed in CD133+ TICs Isolated from Freshly Resected HCC Clinical Specimens

In addition to the five HCC clinical samples used in our initial miRNA assay screening, we also tested the expression of miR-130b in sorted CD133+ TICs and CD133− tumor cells from 15 additional freshly resected HCC patient specimens by qPCR. In addition, miR-130b expression was also examined in CD133+ TICs and CD133− tumor cells that were fractionated by culture as spheroids. miR-130b expression was enriched in the CD133+ subpopulation as compared with the CD133− counterparts (n = 15, $p = 0.018$; Figure 3C). Furthermore, patient-derived spheroids (Figure 3D; data representative of four different tumors tested) that had enriched CD133 expression also displayed enhanced miR-130b as compared with tumor cells that were not CD133+ or their adherent, differentiated counterparts, respectively. PLC8024 HCC spheres that received a mixture of doxorubicin (0.25 μg/ml) and cisplatin (1.6 μg/ml) chemotherapy, drugs commonly used in treating HCC patients clinically, also showed increased miR-130b concomitant with increased CD133 expression, as demonstrated by qPCR analysis (*, $p < 0.05$; Figure 3E).

miR-130b Exhibits an Increased Ability to Proliferate, Self Renew, Form Tumors, and Resist Standard Chemotherapy

We furthered our study to determine how miR-130b regulates the tumorigenicity, self renewal, and chemoresistance of CD133+ TICs. Stable transduction with a lentiviral vector containing the primary transcripts of miR-130b produced high levels of mature miR-130b in Huh7 CD133− or PLC8024 CD133- HCC cells (Figure S2). miR-130b-transduced CD133− HCC cells showed enhanced proliferation compared with control cells transduced with empty vector alone, as measured by XTT cell proliferation assays (*, $p = 0.01$; Figure 4A). CD133− cells transduced with miR-130b also expressed a higher level of stem cell-associated genes, including β-*catenin*, *Notch-1*, *Sox2*, *Nestin*, *Bmi-1*, and ATP-binding cassette half-transporter *ABCG2* (Figure 4B). Moreover, CD133− cells overexpressing miR-130b were also more resistant to the chemotherapeutic drug doxorubicin (Figure 4C). We then examined the effect of increased miR-130b expression on self renewal and tumor growth. CD133− HCC cells with lenti-miR-130b formed bigger and more spheres than CD133− cells carrying only the empty vector lentiviruses in a significantly shorter period of time (Figure 4D). Importantly, miR-130b-transduced spheroids could be passaged from one generation to another, whereas the untransduced spheres could not be passaged. When implanted into the flanks of SCID/Beige mice,

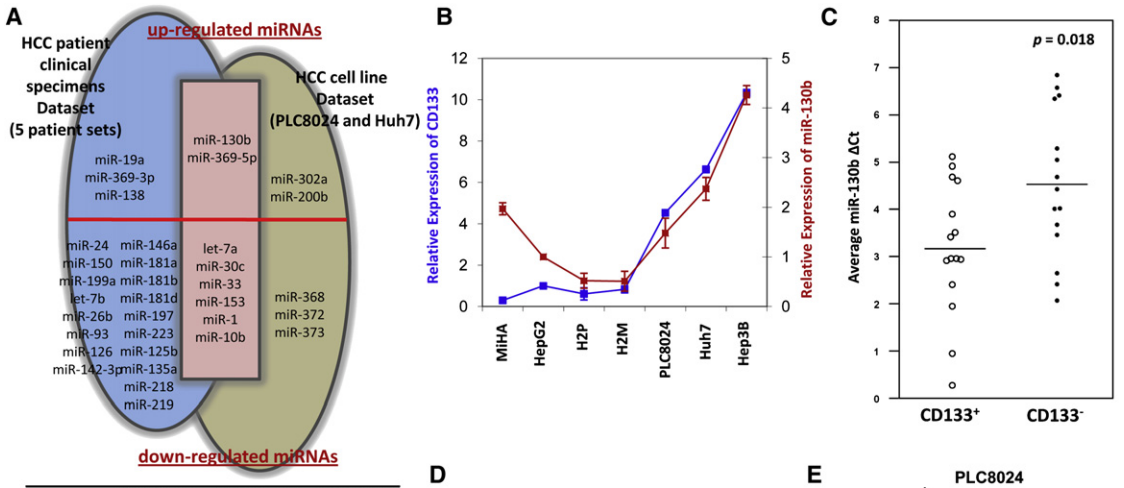

miRNA	Fold change (clinical)	Fold change (Huh7)	Fold change (PLC8024)
Increased Expression			
miR-130b	10.15	3.1325	4.7631
miR-369-5p	5.67	2.8878	2.0676
Decreased Expression			
let-7a	0.014	0.505	0.172
miR-30c	0.219	0.358	0.08
miR-33	0.136	0.844	0.125
miR-153	0.354	0.368	0.47
miR-1	0.188	0.42	0.215
miR-10b	0.078	0.412	0.009

Figure 3. miR-130b Is Preferentially Expressed in CD133+ TICs Isolated from Freshly Resected HCC Clinical Specimens and CD133-Enriched Spheroids

(A) Venn analyses of the up- and downregulated miRNAs in patient-derived HCC samples (left, blue shaded; n = 5 analyzed tumors) and in HCC cell lines PLC8024 and Huh7 (right, beige shaded) are shown. miRNAs that were significantly and commonly deregulated in both patients and cell lines are shown in the overlapping area (pink shaded). Only those miRNAs whose expression levels displayed greater than 0.5-fold decreases or 2-fold increases were further studied. The table shows a summary of the significantly differentially expressed miRNAs in CD133+ compared with CD133− HCC cells with fold change.

(B) CD133 (blue line) and miR-130b (red line) expression positively correlate across a panel of liver cell lines. See also Figure S1.

(C–E) A scatter dot plot shows the increased expression of miR-130b in CD133+ TICs as compared to CD133− counterparts in 15 HCC clinical specimens, as detected by qPCR. qPCR analyses of miR-130b expression in (D) mechanically dissociated cancer spheroids ("sphere") versus primary adherent HCC cells ("diff."), and in (E) PLC8024 HCC spheroids ("sphere") versus their differentiated adherent counterpart ("diff."). were performed following cisplatin (1.6 μg/ml) and doxorubicin (0.25 μg/ml) treatment (*p < 0.05 compared with the differentiated counterpart). Differentiated adherent cells were defined as 1 (calibrator), and the relative expression of miR-130b in the spheroids was expressed as the fold difference over this baseline. β-actin was used as an internal control.

the growth of CD133− cells expressing miR-130b was significantly enhanced (Figure 4E). Of the eight mice per group, miR-130b-transduced CD133− HCC cells (miR-130b) gave rise to tumors in four animals at approximately 9 weeks postinjection, while none of the animals injected with empty vector control CD133− HCC cells (EV) or CD133− cells alone could form tumors (Table 1). Conversely, reducing miR-130b by lentiviral knockdown in PLC8024 CD133+ TICs (ZIP miR-130b) yielded an opposing effect, leading to a reduced ability to form tumors in vivo as compared with CD133+ TICs transduced with antisense controls (ZIP CTRL) or CD133+ TICs alone (Table 1). Similarly, miR-130b-expressing cells gave rise to more tumors when they were serially passaged in vivo into secondary animal recipients (data not shown) and in vitro as tertiary spheroids, suggesting that miR-130b enhances self-renewing capacity (Figure 4F). The tissue structure and cell morphology of tumors generated from CD133+ TICs and CD133− cells expressing miR-130b were not grossly different. Overall, CD133− cells stably expressing miR-130b displayed features more closely resembling CD133+ TICs as compared with CD133- control cells. Conversely, CD133+ cells with miR-130b stably repressed displayed features more closely resembling CD133− cells than CD133+ TICs. The alteration of miR-130b by either lentiviral-enforced or reduced experiments did not alter CD133 expression levels, suggesting that although miR-130b expression was modulated by CD133, a reciprocal inflection was not observed (Figure 4G).

TP53INP1 Is a Direct Target of miR-130b

In an effort to determine the potential downstream mRNA targets regulated by miR-130b, we integrated mRNA expression profiling findings with in silico predictions. Using the latter prediction algorithms of PicTar and TargetScan, we found a total of 289 downstream targets of miR-130b that were common in both algorithms. Microarray analyses of mRNA expression in HCC PLC8024 CD133− cells infected with miR-130b-expressing or empty vectors yielded 271 downregulated genes with a fold change of >2. Overall, with these data sets combined, three

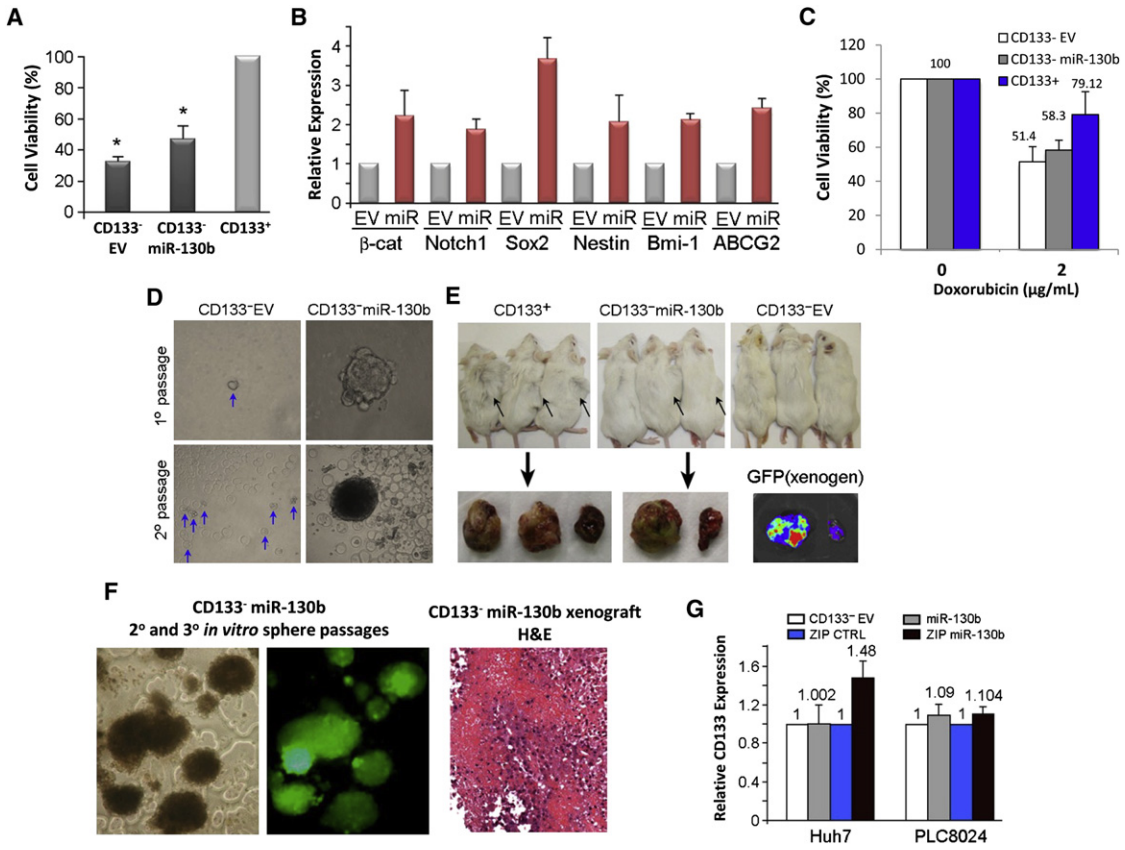

Figure 4. The Role of miR-130b in Regulating Self Renewal, Proliferation, Tumorigenicity, and Chemoresistance in CD133+ TICs Is Shown

(A) Cell proliferation assay was performed for CD133- cells infected with miR-130b-expressing vector or EV (*p = 0.01 compared with CD133+ counterparts).

(B) qPCR analysis was performed for stem cell-associated genes in CD133− cells infected with miR-130b expressing vector (miR) or EV. CD133− cells carrying the EV were defined as 1 (calibrator), and the relative expression of each gene was expressed as the fold difference over this baseline. β-actin was used as an internal control.

(C) The percentages of viable cells from among CD133+ or CD133− cells transduced with miR-130b-expressing vector or EV following treatment of doxorubicin at 0 μg/ml (control) and 2 μg/ml were determined.

(D) CD133− cells expressing miR-130b generated a greater number of spheroids as compared with CD133− cells carrying the EV. The effect of miR-130b on tumor formation in the SCID/Beige mouse xenograft model was determined.

(E) CD133+ or CD133− cells infected with miR-130b-expressing vector or EV were subcutaneously injected into the right posterior flank of each mouse. GFP imaging was done for primary tumors formed by CD133− cells infected with miR-130b using the Xenogen system.

(F) (Left and middle) Serial passages of secondary- and tertiary-generation tumor cells harvested from transplanted mice were subjected to in vitro spheroid formation assays. (Right) Histology panels represent H&E staining of xenografted tumors and confirm a HCC phenotype.

(G) qPCR analysis was performed for CD133 in Huh7 or PLC8024 CD133− cells infected with miR-130b (EV, miR-130b) or for CD133+ cells with antagonized miR-130b (ZIP CTRL, ZIP miR-130b). See also Figure S2.

putative mRNA candidates for miR-130b targeting overlapped: *TP53INP1* (tumor protein p53-inducible nuclear protein 1), *DPYSL2* (dihydropyrimidinase-related protein 2), and *MDFIC* (MyoD family inhibitor domain-containing isoform p40) (Figure 5A and Table S4). Among the three potential targets, we focused on *TP53INP1* because it is a known tumor suppressor gene and because a recent report has demonstrated that TP53INP1 is a functional target of miR-130b in cell-growth dysregulation of human T cell lymphotrophic virus 1 (Yeung et al., 2008).

Base-pairing complementation found that the 3′untranslated region (UTR) of TP53INP1 encompasses two putative binding regions (3927–3953 nt and 5525–5562 nt) bearing significant complementarity against miR-130b (Figure 5B). These two 3′UTR elements of TP53INP1 and miR-130b are extremely conserved among different species, as shown by their identical sequences in mouse, rat, monkey, and human orthologs, suggesting a functional role (Figure 5B). To validate whether TP53INP1 is a bona fide target of miR-130b, a full-length human TP53INP1 3′UTR fragment, as well as two shorter fragments of the TP53INP1 3′UTR encompassing the potential binding regions at positions 3927–3953 nt (site 1) and 5525–5562 nt (site 2), were cloned downstream of the *firefly* luciferase reporter gene. Compared with miR-control experiments, luciferase activity was markedly reduced by approximately 38% in the cells cotransfected with miR-130b and the full-length TP53INP1 3′UTR in the sense orientation. Cells cotransfected with miR-130b and TP53INP1 3′UTR site 1 and/or site 2 also showed reduced luciferase activity by approximately 20%–29% as compared to the miR-control. As a reflection of specificity, this inhibitory effect was abolished when antisense TP53INP1

Table 1. Engraftment Rates of CD133+ and CD133- Subpopulations with or without miR-130b Expression

Cell Type	Tumor Incidence	Cell Number	Latency (days)
CD133+	7/8	10,000	45
	6/8	5,000	51
CD133-	1/8	50,000	70
	1/8	10,000	80
CD133−EV[1]	2/8	10,000	76
	0/8	5,000	-
CD133− miR-130b[1]	4/8	10,000	59
	4/8	5,000	63
CD133+ ZIP CTRL[2]	6/8	10,000	49
	5/8	5,000	55
CD133+ ZIP miR-130b[2]	2/8	10,000	68
	1/8	5,000	82

[1] Overexpression of empty vector (EV) or miR-130b in CD133- cells.
[2] Knockdown of empty vector (ZIP CTRL) or miR-130b (ZIP-miR-130b) in CD133+ cells.

3′UTR site 1 and site 2 constructs were used in place of the sense constructs (Figure 5C). Interestingly, silencing TP53INP1 in PLC8024 CD133− cells did not augment CD133 or miR-130b expression (Figure S3B). In contrast, silencing CD133 in PLC8024 CD133+ (Figure S3A) or Huh7 CD133+ (data not shown) cells significantly repressed miR-130b expression by approximately 10- to 20-fold and concurrently upregulated TP53INP1 expression, suggesting that miR-130b and TP53INP1 are the direct downstream targets of CD133.

Interestingly, the expression of TP53INP1 was inversely correlated with CD133 and miR-130b, at both genomic and proteomic levels, in a series of liver cell lines expressing different CD133 expression levels (Figures 5D, 5E, and S1). Abundant TP53INP1 expression was detected in CD133low HCC cells, like MiHA, H2P and H2M. Conversely, CD133-expressing HCC cells like HepG2, PLC8024, Huh7, and Hep3B expressed low levels, if any at all, of TP53INP1. Likewise, the expression of TP53INP1 was also significantly repressed in CD133+ TICs isolated from freshly resected HCC clinical specimens, as compared with the CD133− HCC counterparts (n = 15, p = 0.043; Figures 5F and 5H). Specifically, in the same 15 matched NT liver and HCC clinical specimens we screened for miR-130b in Figure 3C, a significant inverse correlation was detected between miR-130b and TP53INP1 (p = 0.002, Pearson correlation = −0.732; Figure 5G). The inverse correlation between miR-130b and TP53INP1 in sorted CD133 subpopulations from clinical samples and HCC cell lines was evident at both genomic and proteomic levels (*, p < 0.01; Figures 5H and 5I). In addition, we also observed an inverse TP53INP1 expression following lentiviral upregulation or downregulation of miR-130b expression in CD133− and CD133+ cells, respectively (Figures 5J and 5K).

TP53INP1 Regulates Tumor Formation and Self Renewal in CD133+ TICs

To further examine the role of TP53INP1 in HCC progression, TP53INP1 protein was examined in 17 cases of matched NT and HCC clinical specimens by immunoblot, as well as in a tissue microarray consisting of NT and HCC samples representative of 134 patients. TP53INP1 overexpression in NT was observed in 11 of the 17 (65%) matched cases examined by immunoblot (Patients A, B, C, D, E, I, K, L, M, N and P; Figure 6A). Consistently, the mean TP53INP1 expression in NT was significantly elevated as compared with its corresponding adjacent HCC tissue (n = 77 NT and HCC pairs, Paired t test, p < 0.001) (Figure 6B and Table S5). Intense cytoplasmic staining of TP53INP1 was observed in NT samples (Figure 6B; left), whereas significantly lower expression was found in HCC samples (Figure 6B; right). In addition, high TP53INP1 expression in HCC also correlated with lower AFP levels (χ^2 test, p = 0.019) as well as smaller tumor sizes (χ^2 test, p < 0.001) (Table S5). However, no significant correlation was identified for TP53INP1 expression and gender, age, presence of hepatitis B serum (HBS) antigen and cirrhosis. To further our understanding of the functional role of TP53INP1 in hepatocarcinogenesis, we generated stably repressed TP53INP1 PLC8024 CD133- cells using a shRNA lentiviral knockdown system (Figure 6C). Of the five TP53INP1 shRNA clones, clones 464 and 4095 showed the most dramatic TP53INP1 inhibition compared with nontarget control (NTC) when examined by immunoblot and were thus chosen for further studies (Figure 6C). Repressing TP53INP1 (clones 464 and 4095) in PLC8024 CD133− cells had only a moderate effect on cell proliferation (Figure 6D) but significantly enhanced the ability of the cells to initiate spheroid formation when grown in nonadherent serum-free conditions in vitro and to expand in subsequent in vitro serial propagations (Figure 6E). More interestingly, PLC8024 CD133− cells with repressed TP53INP1 demonstrated an enhanced ability to initiate tumors when injected subcutaneously in immunodeficient animals compared with PLC8024 CD133− NTC cells (Figures 6F and 6H; n = 6 per group, cells injected = 1×10^5). H&E staining of harvested xenografted subcutaneous tumors confirmed a primary HCC phenotype (Figure 6G). Most importantly, primary xenografted tumors formed by PLC8024 CD133− cells with repressed TP53INP1 (clones 464 and 4095) could also self renew, as demonstrated by their ability to serially transplant in secondary mouse recipients. (Figure 6I; n = 5 per group, two groups of cells injected = 1×10^4 and 3×10^4). Serial transplantation of xenografted tumors in secondary animal recipients demonstrated enhanced engraftment ability, as demonstrated by the shorter period of time needed for tumor initiation, as well as by the increase in the number of tumors detected (Figure 6I).

To address whether the above-observed phenotype is indeed due to the suppression of TP53INP1 and not from the targeting of other cellular genes by miR-130b, a rescue experiment was performed. We transduced CD133+ TICs with antagomirs to miR-130b plus shRNA TP53INP1 or with the same antagomirs plus scrambled shRNA controls. Indeed, CD133+ cells with stably repressed miR-130b were enhanced in both spheroid formation ability and self-renewal ability and showed increased tumorigenicity in immunodeficient mice when shRNA TP53INP1, but not the scrambled shRNA control, was cotransfected (Figures 6J and 6K). Like CD133+ and CD133+ ZIP CTRL, CD133+ cells stably repressed with miR-130b and transfected with TP53INP1 could similarly initiate spheroid formation and expand in subsequent serial propagations (Figure 6J). These cells also displayed a similar ability to initiate tumors when

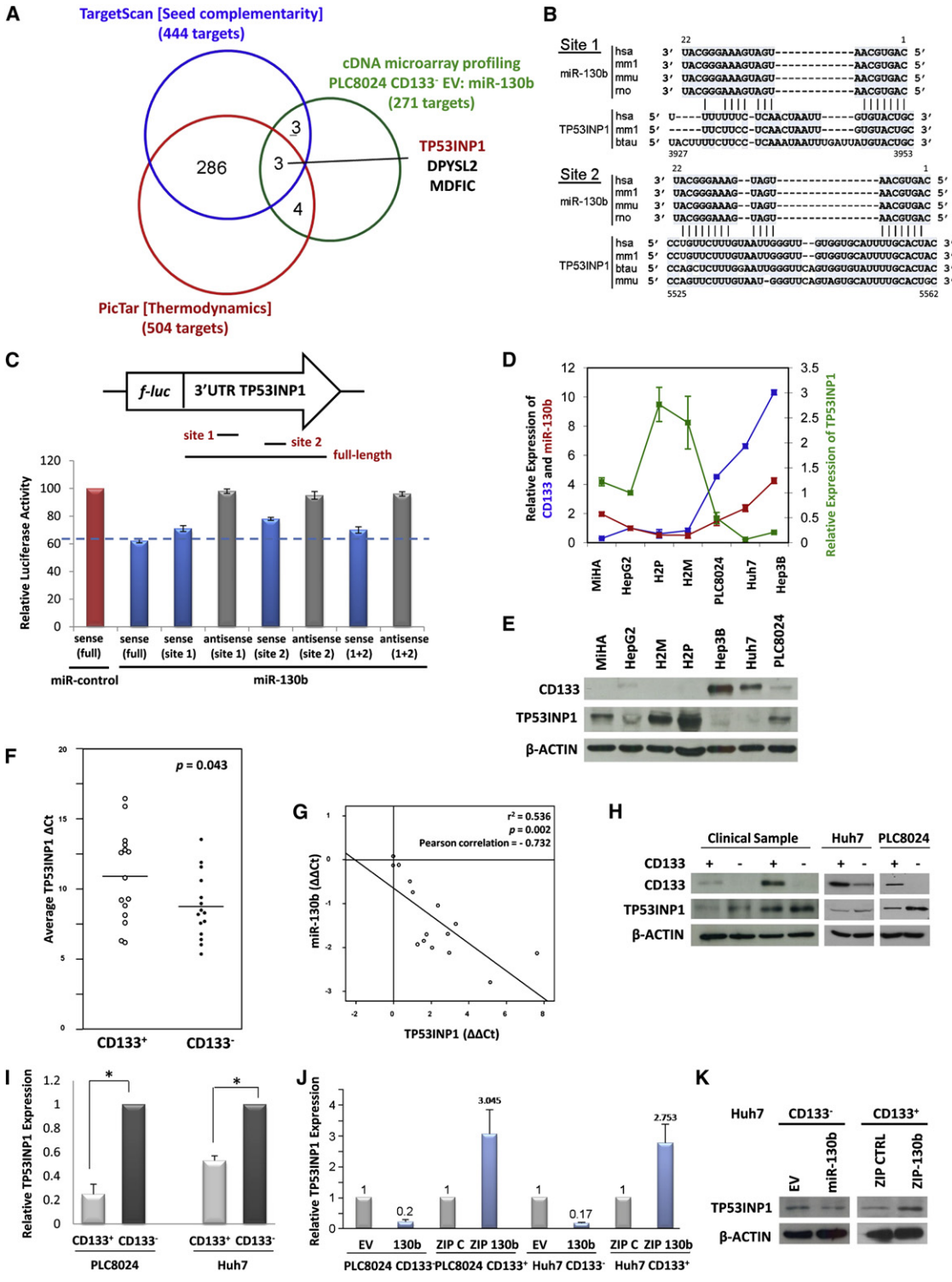

Figure 5. TP53INP1 Is a Direct Target of miR-130b

(A) A Venn diagram displays candidate mRNAs that were computationally predicted to be targeted by miR-130b by PicTar (red), TargetScan (blue) and mRNA expression profiling (green). See also Table S4.

(B) The mouse (mmu: *Mus musculus*), rat (rno: *Rattus norvegicus*), monkey (mml: *Macaca mulatta*), cow (btau: *Bos taurus*) and human (hsa: *Homo sapiens*) miR-130b and the two predicted miR-130b binding sites in the 3′UTR of TP53INP1 at nt 3927-3953 and nt 5525-5562 in different species were checked for alignment. The positions of the miRNA binding sites corresponded to the location of the GenBank sequence NM_033285.

(C) An analysis of luciferase activity was performed. The full-length 3′UTR of TP53INP1 (full-length) and two shorter fragments of TP53INP1 3′UTR encompassing the potential binding regions (site 1 at nt 3927-3953 and site 2 at nt 5525-5562) were PCR-amplified and then cloned downstream of a *firefly* luciferase gene. The

injected subcutaneously in immunodeficient animals as compared to CD133+ and CD133+ ZIP CTRL cells (Figure 6K; n = 3 per group, mice sacrificed at 12 weeks). For better comparison, experiments were carried out alongside CD133− and CD133+ ZIP miR-130b cells.

DISCUSSION

Epithelial tumors are made up of a heterogeneous population of cells at multiple differentiation stages. This cellular heterogeneity can be characterized by differences in the histopathologies, clinical behaviors, molecular profiles, and functional properties. Some studies suggest that such intratumoral heterogeneity may arise from acquired mutations and epigenetic differences of tumor cells through selective pressure during tumor evolution. Recently, increasing evidence has lent support to the notion that at the apex of this heterogeneous population of cells is a TIC population that orchestrates aberrant differentiation, thereby resulting in the observed cellular and functional heterogeneity of epithelial tumors (Pardal et al., 2003). The origin of these cells is unknown, but TICs may arise by mutations from normal stem cells that retain self-renewal properties but acquire genetic and/or epigenetic mutations, resulting in cancerous stem cells. In contrast, TICs could also arise from mutated progenitors or more committed differentiated cells that acquire the self-renewal capacity and immortality typifying TICs.

Our current data show that HCC is driven by a small population of TICs expressing the CD133 stem cell marker. Our data are well in line with the TIC hypothesis suggesting that tumors are generated and maintained by a small subset of cells with the ability to self renew and differentiate into the bulk tumor population. To date, the TIC hypothesis has been proven in a wide variety of solid tumors, including breast, brain, colorectal, head and neck, pancreatic, prostate, melanoma, and liver cancers (Visvader and Lindeman, 2008). In addition, these results also agree with our past studies where we identified a group of primitive stem/progenitor cells from HCC cell lines and xenograft tumors that is marked by a CD133 surface phenotype and bears features including the ability to self renew, differentiate, and initiate tumors in vivo and resist standard chemotherapy (Ma et al., 2007, 2008). Likewise, using HCC cell lines, a few other groups have also found liver TICs to be identified by the CD133 surface phenotype (Suetsugu et al., 2006; Yin et al., 2007; Zhu et al., 2010; Song et al., 2008). To our knowledge, this is the first study to identify CD133 as a marker of liver TICs from freshly resected tumor specimens and, most importantly, is one of the few studies to associate CD133 expression in HCC with an advanced tumor stage, a larger tumor size, and a poor prognosis.

CD133 is expressed by normal tissue-resident as well as malignant stem cells of the hematopoietic, neural, pancreatic, colonic, and endothelial lineages. CD133 is expressed on early stem/progenitors but is usually no longer detectable upon differentiation. Thus, our previous and present data from HCC also correspond with these earlier findings where we identified a subpopulation of CD133+ cells in a murine liver regenerating model in which 70% of the liver was removed and a subpopulation of CD133+ cells that bear self-renewal capacity because they can be clonally expanded, are exclusively tumorigenic, and can differentiate into CD133− cells (Ma et al., 2007). A couple of recent studies in HCC have utilized CD90+CD44+ (Yang et al., 2008) and EpCAM+ (Yamashita et al., 2009) for the identification of TICs. Our preliminary data suggest that the expressions of EpCAM and CD133 do overlap in some HCC tissue specimens and cell lines but are not identical, while CD90 is undetectable in these cells.

Following the identification of CD133 in liver TICs in the first part of our study, the next step was to characterize the underlying molecular and biological mechanisms by which these cells mediate tumor formation and growth. To date, the mechanisms regulating these cells remain obscure. Thus, in the second part of our study, we examined whether differences in miRNA expression could distinguish CD133+ HCC TICs from their more differentiated progeny. Sorted CD133 subpopulations from HCC clinical specimens and HCC cell lines were profiled for the expression of 95 miRNAs. A significant overexpression of miR-130b distinguishes CD133+ TICs from their differentiated progeny. miR-130b was preferentially expressed in CD133+ spheres derived from HCC clinical samples as well as chemotherapy-treated unsorted spheres enriched for CD133. Functional studies found that miR-130b was required for self renewal in vitro, tumorigenicity in vivo, and chemoresistance. The overexpression of miR-130b in CD133− cells enhanced proliferation, displayed superior resistance to chemotherapeutic agents, elevated the expression of stem cell-associated genes, and gave enhanced tumorigenicity in vivo and greater potential for self renewal in serial passages than when compared with control cells transduced with empty vector alone. Conversely, the

specificity of the inhibition was determined using antisense constructs (3′-5′ orientation). The pRL-TK *Renilla* luciferase plasmid was cotransfected as a normalization control for *firefly* luciferase activity. The inverse correlation of miR-130b and TP53INP1 expression in HCC clinical samples and cell lines is shown.

(D) The inverse correlations of CD133 (blue line) and miR-130b (red line) against TP53INP1 (green line) expression were determined across a panel of liver cell lines. See also Figure S1.

(E) Immunoblots of the same series of HCC cell lines were performed for CD133 and TP53INP1 expression determinations. β-actin was used an as internal loading control.

(F) A scatter dot-plot showed decreased expression of TP53INP1 in CD133+ TICs as compared to the CD133- counterparts in 15 HCC clinical specimens, as detected by qPCR.

(G-I) The inverse correlation between miR-130b and TP53INP1 expression in CD133+ versus CD133- subpopulations in 15 HCC clinical samples was determined with linear regression lines and Pearson correlation significance. TP53INP1 expression in CD133+ and CD133- cells from freshly resected tumors and HCC cell lines was analyzed by both (H) immunoblot and (I) qPCR analysis. For qPCR, CD133- cells of each sample were defined as 1 (calibrator), and the relative expression of TP53INP1 in CD133+ TICs was expressed as the fold difference over this baseline level (*$p < 0.01$). β-actin was used as an internal control.

(J and K) qPCR (J) and immunoblots (K) were used to examine the expression of TP53INP1 in CD133- cells infected with miR-130b-expressing vector or EV and in CD133+ cells infected with ZIP miR-130b-expressing vector or ZIP control (CTRL). Increased and suppressed expressions of endogenous TP53INP1 by knockdown and overexpression of miR-130b were detected, respectively. See also Figure S3.

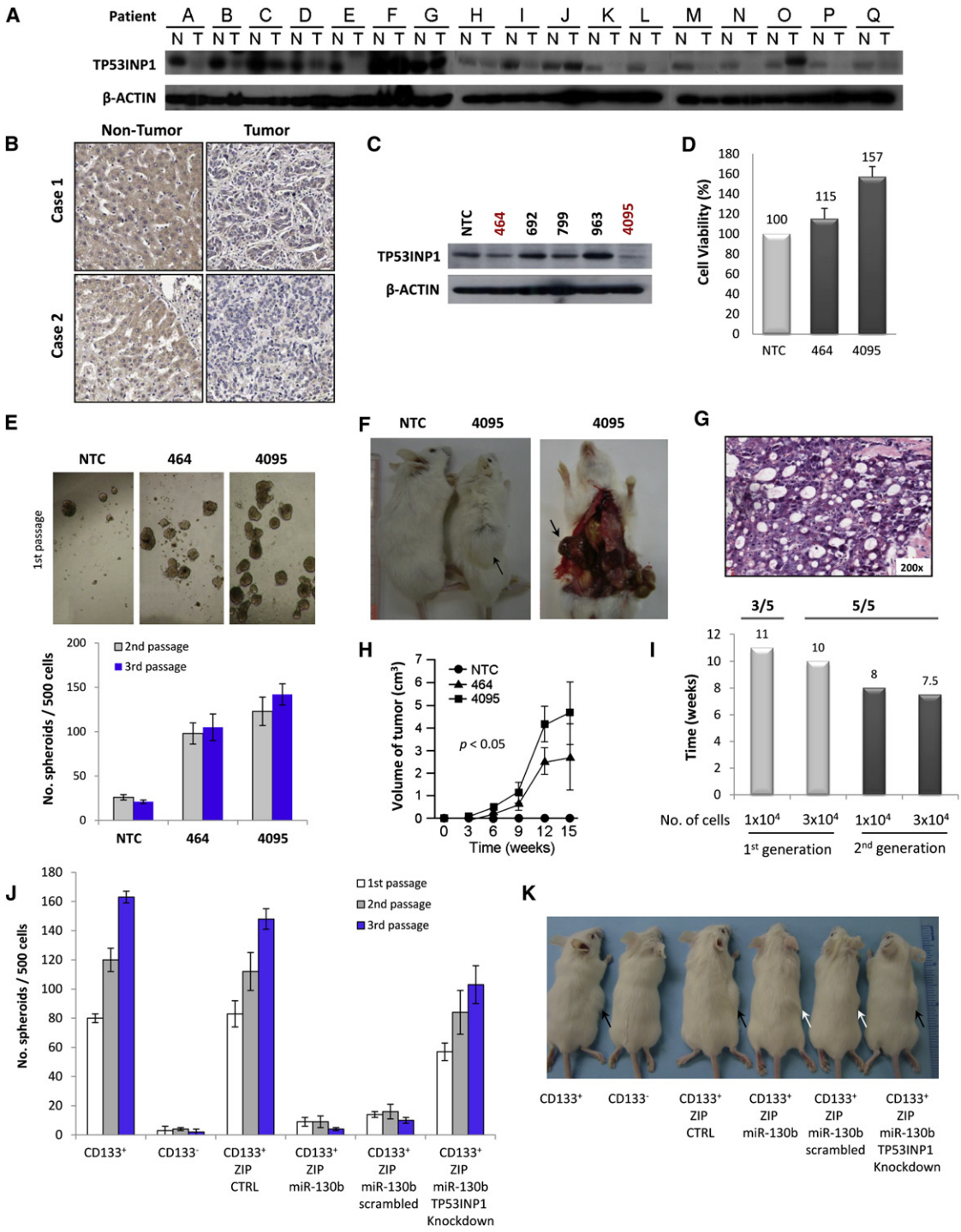

Figure 6. TP53INP1 Regulates Tumor Formation and Self Renewal in CD133⁺ TICs

(A) TP53INP1 expression was determined in 17 cases of matched NT and HCC (Patients A to Q) by immunoblot. β-actin was used an as internal loading control.

(B) IHC staining for TP53INP1 expression was performed in a tissue microarray consisting of NT and HCC samples representative of 134 patients. Representative images of TP53INP1 overexpression in NT compared to the matched HCC counterparts are shown. Intense cytoplasmic staining of TP53INP1 was observed in NT (left), whereas HCC showed little or no staining (right). IHC images were taken at a 200× magnification. See also Table S5.

(C) Immunoblot analysis for TP53INP1 expression in PLC8024 CD133⁻ cells following shRNA TP53INP1 stable knockdown determined that clones 464 and 4095 significantly repress TP53INP1 expression compared with NTC. β-actin was used an as internal loading control.

(D) The knockdown of TP53INP1 in PLC8024 CD133⁻ cells (clones 464 and 4095) resulted in moderate augmentation in cell proliferation compared with NTC.

(E) PLC8024 CD133⁻ cells with repressed TP53INP1 (clones 464 and 4095) generated a greater number of spheroids (top) and could be serially passaged (bottom) as compared with NTCs.

antagonization of miR-130b in CD133+ cells resulted in an opposite effect.

By integrated analyses through mRNA expression profiling and in silico predictions, we identified TP53INP1 as a functional downstream target of miR-130b. Five lines of evidence support this finding. First, there are two highly conserved miR-130b binding sites in the 3′UTR of TP53INP1. Second, the stable overexpression or knockdown of miR-130b reduced or enhanced TP53INP1 levels, respectively, at both the mRNA and protein levels, in a number of HCC cell lines. Third, expression of miR-130b and TP53INP1 were found to be significantly inversely correlated in HCC clinical specimens. Fourth, TP53INP1 3′UTR-mediated luciferase activity is specifically responsive to transduced miR-130b. Fifth, a rescue experiment where CD133+ cells that stably repressed miR-130b with overexpressed TP53INP1 expression and dually transfected with shRNA TP53INP1, successfully enhanced the cells' ability to grow and self renew. TP53INP1 is a proapoptotic stress-induced p53 target gene. It is a tumor suppressor gene with a known role in cellular homeostasis through its antiproliferative and proapoptotic activities via both p53-dependent and p53-independent means (Tomasini et al., 2001; Tomasini et al., 2002; Okamura et al., 2001). It is an alternatively spliced gene encoding two protein isoforms (TP53INP1α and TP53INP1β), and when overexpressed, both isoforms exert a tumor suppressor function, mainly by inducing the transcription of target genes involved in cell-cycle arrest and p53-mediated apoptosis as part of the cell response to genotoxic stress. Findings in recent years have shown a significant reduction or loss of TP53INP1 expression during the development of cancers of the stomach (Jiang et al., 2006), breast (Ito et al., 2006), and pancreas (Gironella et al., 2007). Mice deficient for TP53INP1 also present with exacerbated colitis-associated carcinogenesis (Gommeaux et al., 2007). In addition, TP53INP1 expression was lost in rat preneoplastic lesions in the liver (Ogawa et al., 2005). Recently, miR-130b was found to work as a tumor suppressor by silencing TP53INP1 in human T cell leukemia (Yeung et al., 2008). Our data in the last part of this paper found that miR-130b-induced downregulation of TP53INP1 promotes tumor growth and self renewal in CD133+ TICs. TP53INP1 expression determinations on a tissue microarray consisting of NT and HCC specimens and by immunoblot found that TP53INP1 was significantly downregulated in HCC as compared with NT tissue. Silencing TP53INP1 in PLC8024 CD133− cells enhanced both spheroid formation and tumorigenicity in immunodeficient mice as well as self renewal as evident by serial transplantation. Further, a rescue experiment found CD133+ TICs transduced with antagomirs to miR-130b plus shRNA TP53INP1, but not scrambled shRNA control, enhanced ability of the cells to form spheres, to develop tumors in immunodeficient mice, as well as to self-renew. miR-130b thus acts as a regulator of stemness and tumorigenicity by silencing TP53INP1.

Clinically, the relevance of TICs has become more evident, underscoring the importance of this theory and the need for the better characterization of these cells. The characterization of molecular targets downstream of CD133+ liver TICs in this study not only will allow for better understanding of the mechanisms regulating this specific population of cells but also will provide insight into the gradual improvement of more effective cancer therapies against this disease.

EXPERIMENTAL PROCEDURES

Fresh Clinical Tissue Specimens

Fresh human liver tumor and adjacent NT tissue specimens were obtained in accordance with the ethical standards of the institutional committee on human experimentation from 83 patients undergoing hepatectomy for HCC. Specimens were collected between 2008 and 2009 at the Queen Mary Hospital or the Prince of Wales Hospital in Hong Kong. No previous local or systemic treatment had been conducted for these patients prior to operation. Histological examination was carried out by pathologists, and diagnosis was made based on the microscopic features of the carcinoma cells. Tumors were graded using the American Joint Committee on Cancer (AJCC)/International Union Against Cancer (UICC) tumor staging system. Surgical specimens were obtained at the time of resection from all patients. All samples were received in the laboratory within 20 min, immediately mechanically disaggregated and digested with type IV collagenase (Sigma-Aldrich; Louis, MO), and then resuspended in DMEM/F12 medium containing penicillin (500 U/ml) and streptomycin (500 μg/ml). Single-cell suspensions were obtained by filtration through a 100 μm filter (BD Biosciences; Franklin Lakes, NJ). Dead cells and red blood cells were removed using the Ficoll gradient centrifugation method. Remaining red blood cells were lysed with ACK buffer (Invitrogen; Carlsbad, CA). The number of viable cells was counted and analyzed using trypan blue staining.

Clinical Samples for CD133 Survival Correlation Studies

Liver tumor tissue specimens were obtained from 41 patients who underwent liver resection for HCC between 2000 and 2005 at the Queen Mary Hospital in Hong Kong. The patients included 37 men and 4 women with ages ranging from 28 to 80 years (median: 55 years). Tumors were graded using the AJCC/UICC tumor staging system. The clinical information of the patients is summarized in Table S1. Informed consent was obtained from all patients before the collection of liver specimens, and the study was approved by the Ethics Committee of the University of Hong Kong.

Cell Sorting and Flow Cytometry

Cell sorting by flow cytometry was performed on liver cells using PE-conjugated monoclonal mouse anti-human CD133/1 (AC133, Miltenyi Biotec; Auburn, CA). Isotype control mouse IgG1κ-PE (eBioscience; San Diego, CA) served as a control. Samples were analyzed and sorted on a BD FACSVantage SE (BD Biosciences). Only the top 25% most brightly stained or the bottom 20% most dimly stained cells were selected as positive and negative populations, respectively. Magnetic cell separation was performed on tumor cell populations obtained from enzymatic dissociation of HCC specimens using microbeads conjugated with CD133/1 (AC133, Cell Isolation Kit, Miltenyi Biotec). Magnetic separation was performed twice. The quality of sorting

(F) Representative images are shown for the tumors (black arrow, subcutaneous tumor) formed in SCID/Beige mice by PLC8024 CD133− cells infected with shRNA TP53INP1 clones 464 and 4095 or NTC when injected subcutaneously in the right posterior flank (n = 6 per group).
(G) Histology panels representing H&E staining of harvested tumors confirmed a primary HCC phenotype.
(H) Tumor volumes were measured after tumor cell inoculation every 10 days for a period of 15 weeks.
(I-K) Serial transplantation of xenografted TP53INP1 clone 4095 tumors in secondary animal recipients (n = 5 per group) demonstrated enhanced engraftment ability, as demonstrated by the shorter period of time needed for tumor initiation and the increased number of tumors detected. The number of tumors detected/number of mice injected is shown above the bars. The suppression of TP53INP1 in CD133+ TICs with stably repressed miR-130b resulted in a rescue of (J) its ability to form spheroids in primary (white column), secondary (gray column) and tertiary passages (blue column) as well as (K) its ability to form tumors in immunodeficient mice (n = 3 per group). Black arrows depict larger tumors, and white arrows depict smaller tumors.

was controlled by flow cytometry with an antibody against a different CD133 epitope (CD133/2, AC141, Miltenyi Biotec). Viability was assessed using trypan blue exclusion. Sorted and unsorted cells from human specimens and xenografts were analyzed for CD133 expression using PE-conjugated CD133/1 (AC133, Miltenyi Biotec) and isotype control mouse IgG1κ-PE (eBioscience). $CD133^+$ sorted cells were analyzed for panendothelial CD31 and panleukocyte CD45 expression using FITC-conjugated monoclonal mouse anti-human CD31 (eBioscience) and FITC-conjugated monoclonal mouse anti-human CD45 (clone 2D1, Stem Cell Technologies) or isotype control mouse IgG1κ-FITC (eBioscience). Flow cytometry was performed on a FACSCalibur apparatus, and data were analyzed using CellQuest software (BD Biosciences).

miRNA Profiling

miRNA expression profiling was performed using total RNA with the Stem Cell miRNA qPCR Array (System Biosciences; Mountain View, CA), which simultaneously profiles 95 different human miRNAs with potential roles in cellular self renewal and differentiation. Human small nuclear U6 RNA was amplified as a normalization control. All miRNAs were registered with the Sanger miRBase database. qPCR was performed using SYBR Green as mentioned above. The analysis was performed using software provided by System Biosciences.

Animal Model and Animal Charge-Couple Device Experiments

The study protocol was approved by and performed in accordance with the Committee of the Use of Live Animals in Teaching and Research at the University of Hong Kong. Tumorigenicity was determined by orthotopic injection into the liver or subcutaneous injection into the flank of 4-to-5-week old SCID/Beige mice. For orthotopic injections, single dissociated cells from freshly resected tumors were sorted for $CD133^+$ and $CD133^-$ cells and were injected orthotopically into the liver in a mixture of complete medium and Matrigel (BD Biosciences) at a 1:1 ratio. For miR-130b transplantation studies, $CD133^+$ TICs infected with antagomirs to miR-130b or antisense control or $CD133^-$ cells infected with miR-130b or empty vector were injected subcutaneously in complete medium. Each group contained eight animals. After tumors were detected, tumor sizes were measured every 3 days by calipers, and tumor volumes were calculated as volume (cm^3) = $L \times W^2 \times 0.5$. Harvested tumors were imaged immediately after sacrifice. Briefly, imaging was done using a Xenogen IVIS 100 cooled charge-coupled device camera (Caliper Life Sciences; Hopkinton, MA). The acquisition time ranged from 30 s to 1 min. A gray-scale reference image was obtained, followed by the acquisition of a bioluminescent image. The images shown are pseudoimages of the emitted light in photons/s/cm^2/steradian superimposed over the gray-scale photographs of the animal. For TP53INP1 transplantation studies, lentiviral-delivered shRNA TP53INP1 or shRNA nontarget control $CD133^-$ cells were injected subcutaneously in complete medium. Each group contained five or six animals. Cryosections (5 μm thick) were stained with H&E and used for IHC. Animals that were injected with tumor cells but showed no sign of tumor burden were generally terminated 5 months after tumor cell inoculation, and animals were opened up at the injection sites to confirm that there was no tumor development.

Statistical Analysis

All statistical analyses were performed using PASW Statistics 18.0 (SPSS, Inc.; Chicago, IL), with the exception of the significance in bar graphs, in which case analyses were performed by applying the independent t test using Microsoft Office Excel software (Microsoft Corp.; Redmond, WA). A p value of less than 0.05 was considered significant. Differences in CD133 expression among different clinicopathological stages were analyzed by Chi-square (χ^2) test. Cases with ΔCt values falling within the range of half standard deviation (SD) plus or minus the mean value (10.36 ± 1.6) were excluded from the analysis. Cases with ΔCt lower than the mean value minus half of the SD were classified as having high CD133 expression, while cases with ΔCt higher than the mean value plus half of the SD were classified as having low CD133 expression. The Kaplan-Meier method and the log-rank test were used to compare the survival, defined as the time from surgery until death (living patients were censored at the time of their last follow up), of patients with $CD133^+$ and patients with $CD133^-$ primary tumors. For the calculation of differences in the mean score of TP53INP1 in the NT versus HCC tissue microarrays, only 77 of the 134 patients were included in the paired t test calculation. The remaining 57 patients were negative for TP53INP1 in either NT or T and thus had to be excluded.

SUPPLEMENTAL INFORMATION

Supplemental Information includes three figures, five tables, Supplemental Experimental Procedures, and Supplemental References and can be found with this article online at doi:10.1016/j.stem.2010.11.010.

ACKNOWLEDGMENTS

The authors would like to thank Dr. Alice Carrier (INSERM; France) for her gift of the monoclonal rat anti-human TP53INP1 (E12) antibody, Drs. Man Lung Yeung and Kuan-The Jeang (NIH; USA) for their gift of the full-length 3′UTR TP53INP1 plasmid, Mr. Fai Ng (University of Hong Kong, HK) for his expert assistance with the cell-sorting facility and Professor George Tsao (Centre for Cancer Research, University of Hong Kong, HK) for his support on cancer stem cell studies. This work was generously supported by Sir Michael and Lady Kadoorie Funded Research into Cancer Genetics, Research Grant Council Collaborative Research Fund (HKU 1/06C, HKU 7/CRG/09 and HKU5/CRF/08), National Key Sci-Tech Special Project of Infectious Diseases (2008ZX1002-022), The University of Hong Kong Strategic Research Theme in Cancer, The University of Hong Kong Seed Funding Program, The University of Hong Kong Small Project Funding Program, and Donation of the Li Ka Shing Foundation of Matching Grants of The University of Hong Kong.

Received: January 14, 2010
Revised: July 9, 2010
Accepted: September 2, 2010
Published: December 2, 2010

REFERENCES

Aravalli, R.N., Steer, C.J., and Cressman, E.N. (2008). Molecular mechanisms of hepatocellular carcinoma. Hepatology *48*, 2047–2063.

Bernstein, E., Kim, S.Y., Carmell, M.A., Murchison, E.P., Alcorn, H., Li, M.Z., Mills, A.A., Elledge, S.J., Anderson, K.V., and Hannon, G.J. (2003). Dicer is essential for mouse development. Nat. Genet. *35*, 215–217.

Calin, G.A., Ferracin, M., Cimmino, A., Di Leva, G., Shimizu, M., Wojcik, S.E., Iorio, M.V., Visone, R., Sever, N.I., Fabbri, M., et al. (2005). A MicroRNA signature associated with prognosis and progression in chronic lymphocytic leukemia. N. Engl. J. Med. *353*, 1793–1801.

Chen, J.F., Murchison, E.P., Tang, R., Callis, T.E., Tatsuguchi, M., Deng, Z., Rojas, M., Hammond, S.M., Schneider, M.D., Selzman, C.H., et al. (2008). Targeted deletion of Dicer in the heart leads to dilated cardiomyopathy and heart failure. Proc. Natl. Acad. Sci. USA *105*, 2111–2116.

Croce, C.M., and Calin, G.A. (2005). miRNAs, cancer, and stem cell division. Cell *122*, 6–7.

Davis, T.H., Cuellar, T.L., Koch, S.M., Barker, A.J., Harfe, B.D., McManus, M.T., and Ullian, E.M. (2008). Conditional loss of Dicer disrupts cellular and tissue morphogenesis in the cortex and hippocampus. J. Neurosci. *28*, 4322–4330.

DeSano, J.T., and Xu, L. (2009). MicroRNA regulation of cancer stem cells and therapeutic implications. AAPS J. *11*, 682–692.

Esquela-Kerscher, A., and Slack, F.J. (2006). Oncomirs - microRNAs with a role in cancer. Nat. Rev. Cancer *6*, 259–269.

Filipowicz, W., Bhattacharyya, S.N., and Sonenberg, N. (2008). Mechanisms of post-transcriptional regulation by microRNAs: are the answers in sight? Nat. Rev. Genet. *9*, 102–114.

Gangaraju, V.K., and Lin, H. (2009). MicroRNAs: key regulators of stem cells. Nat. Rev. Mol. Cell Biol. *10*, 116–125.

Gironella, M., Seux, M., Xie, M.J., Cano, C., Tomasini, R., Gommeaux, J., Garcia, S., Nowak, J., Yeung, M.L., Jeang, K.T., et al. (2007). Tumor protein 53-induced nuclear protein 1 expression is repressed by miR-155, and its restoration inhibits pancreatic tumor development. Proc. Natl. Acad. Sci. USA *104*, 16170–16175.

Gommeaux, J., Cano, C., Garcia, S., Gironella, M., Pietri, S., Culcasi, M., Pébusque, M.J., Malissen, B., Dusetti, N., Iovanna, J., and Carrier, A. (2007). Colitis and colitis-associated cancer are exacerbated in mice deficient for tumor protein 53-induced nuclear protein 1. Mol. Cell. Biol. *27*, 2215–2228.

Hatfield, S.D., Shcherbata, H.R., Fischer, K.A., Nakahara, K., Carthew, R.W., and Ruohola-Baker, H. (2005). Stem cell division is regulated by the microRNA pathway. Nature *435*, 974–978.

He, L., and Hannon, G.J. (2004). MicroRNAs: small RNAs with a big role in gene regulation. Nat. Rev. Genet. *5*, 522–531.

Inui, M., Martello, G., and Piccolo, S. (2010). MicroRNA control of signal transduction. Nat. Rev. Mol. Cell Biol. *11*, 252–263.

Iorio, M.V., Ferracin, M., Liu, C.G., Veronese, A., Spizzo, R., Sabbioni, S., Magri, E., Pedriali, M., Fabbri, M., Campiglio, M., et al. (2005). MicroRNA gene expression deregulation in human breast cancer. Cancer Res. *65*, 7065–7070.

Ito, Y., Motoo, Y., Yoshida, H., Iovanna, J.L., Takamura, Y., Miya, A., Kuma, K., and Miyauchi, A. (2006). Decreased expression of tumor protein p53-induced nuclear protein 1 (TP53INP1) in breast carcinoma. Anticancer Res. *26* (6B), 4391–4395.

Jemal, A., Siegel, R., Ward, E., Hao, Y., Xu, J., and Thun, M.J. (2009). Cancer statistics, 2009. CA Cancer J. Clin. *59*, 225–249.

Ji, J., Yamashita, T., Budhu, A., Forgues, M., Jia, H.L., Li, C., Deng, C., Wauthier, E., Reid, L.M., Ye, Q.H., et al. (2009). Identification of microRNA-181 by genome-wide screening as a critical player in EpCAM-positive hepatic cancer stem cells. Hepatology *50*, 472–480.

Jiang, P.H., Motoo, Y., Garcia, S., Iovanna, J.L., Pébusque, M.J., and Sawabu, N. (2006). Down-expression of tumor protein p53-induced nuclear protein 1 in human gastric cancer. World J. Gastroenterol. *12*, 691–696.

Jiang, J., Gusev, Y., Aderca, I., Mettler, T.A., Nagorney, D.M., Brackett, D.J., Roberts, L.R., and Schmittgen, T.D. (2008). Association of MicroRNA expression in hepatocellular carcinomas with hepatitis infection, cirrhosis, and patient survival. Clin. Cancer Res. *14*, 419–427.

Jordan, C.T., Guzman, M.L., and Noble, M. (2006). Cancer stem cells. N. Engl. J. Med. *355*, 1253–1261.

Koralov, S.B., Muljo, S.A., Galler, G.R., Krek, A., Chakraborty, T., Kanellopoulou, C., Jensen, K., Cobb, B.S., Merkenschlager, M., Rajewsky, N., and Rajewsky, K. (2008). Dicer ablation affects antibody diversity and cell survival in the B lymphocyte lineage. Cell *132*, 860–874.

Ma, S., Chan, K.W., Hu, L., Lee, T.K., Wo, J.Y., Ng, I.O., Zheng, B.J., and Guan, X.Y. (2007). Identification and characterization of tumorigenic liver cancer stem/progenitor cells. Gastroenterology *132*, 2542–2556.

Ma, S., Lee, T.K., Zheng, B.J., Chan, K.W., and Guan, X.Y. (2008). CD133+ HCC cancer stem cells confer chemoresistance by preferential expression of the Akt/PKB survival pathway. Oncogene *27*, 1749–1758.

Ogawa, K., Asamoto, M., Suzuki, S., Tsujimura, K., and Shirai, T. (2005). Downregulation of apoptosis revealed by laser microdissection and cDNA microarray analysis of related genes in rat liver preneoplastic lesions. Med. Mol. Morphol. *38*, 23–29.

Okamura, S., Arakawa, H., Tanaka, T., Nakanishi, H., Ng, C.C., Taya, Y., Monden, M., and Nakamura, Y. (2001). p53DINP1, a p53-inducible gene, regulates p53-dependent apoptosis. Mol. Cell *8*, 85–94.

Pardal, R., Clarke, M.F., and Morrison, S.J. (2003). Applying the principles of stem-cell biology to cancer. Nat. Rev. Cancer *3*, 895–902.

Reinhart, B.J., Slack, F.J., Basson, M., Pasquinelli, A.E., Bettinger, J.C., Rougvie, A.E., Horvitz, H.R., and Ruvkun, G. (2000). The 21-nucleotide let-7 RNA regulates developmental timing in Caenorhabditis elegans. Nature *403*, 901–906.

Shimono, Y., Zabala, M., Cho, R.W., Lobo, N., Dalerba, P., Qian, D., Diehn, M., Liu, H., Panula, S.P., Chiao, E., et al. (2009). Downregulation of miRNA-200c links breast cancer stem cells with normal stem cells. Cell *138*, 592–603.

Song, W., Li, H., Tao, K., Li, R., Song, Z., Zhao, Q., Zhang, F., and Dou, K. (2008). Expression and clinical significance of the stem cell marker CD133 in hepatocellular carcinoma. Int. J. Clin. Pract. *62*, 1212–1218.

Suetsugu, A., Nagaki, M., Aoki, H., Motohashi, T., Kunisada, T., and Moriwaki, H. (2006). Characterization of CD133+ hepatocellular carcinoma cells as cancer stem/progenitor cells. Biochem. Biophys. Res. Commun. *351*, 820–824.

Suh, M.R., Lee, Y., Kim, J.Y., Kim, S.K., Moon, S.H., Lee, J.Y., Cha, K.Y., Chung, H.M., Yoon, H.S., Moon, S.Y., et al. (2004). Human embryonic stem cells express a unique set of microRNAs. Dev. Biol. *270*, 488–498.

Tomasini, R., Samir, A.A., Vaccaro, M.I., Pebusque, M.J., Dagorn, J.C., Iovanna, J.L., and Dusetti, N.J. (2001). Molecular and functional characterization of the stress-induced protein (SIP) gene and its two transcripts generated by alternative splicing. SIP induced by stress and promotes cell death. J. Biol. Chem. *276*, 44185–44192.

Tomasini, R., Samir, A.A., Pebusque, M.J., Calvo, E.L., Totaro, S., Dagorn, J.C., Dusetti, N.J., and Iovanna, J.L. (2002). P53-dependent expression of the stress-induced protein (SIP). Eur. J. Cell Biol. *81*, 294–301.

Ura, S., Honda, M., Yamashita, T., Ueda, T., Takatori, H., Nishino, R., Sunakozaka, H., Sakai, Y., Horimoto, K., and Kaneko, S. (2009). Differential microRNA expression between hepatitis B and hepatitis C leading disease progression to hepatocellular carcinoma. Hepatology *49*, 1098–1112.

Visvader, J.E., and Lindeman, G.J. (2008). Cancer stem cells in solid tumors: accumulating evidence and unresolved questions. Nat. Rev. Cancer *10*, 755–768.

Wang, Y., Medvid, R., Melton, C., Jaenisch, R., and Blelloch, R. (2007). DGCR8 is essential for microRNA biogenesis and silencing of embryonic stem cell self-renewal. Nat. Genet. *39*, 380–385.

Yamashita, T., Ji, J., Budhu, A., Forgues, M., Yang, W., Wang, H.Y., Jia, H., Ye, Q., Qin, L.X., Wauthier, E., et al. (2009). EpCAM-positive hepatocellular carcinoma cells are tumor-initiating cells with stem/progenitor cell features. Gastroenterology *136*, 1012–1024.

Yang, Z.F., Ho, D.W., Ng, M.N., Lau, C.K., Yu, W.C., Ngai, P., Chu, P.W., Lam, C.T., Poon, R.T., and Fan, S.T. (2008). Significance of CD90+ cancer stem cells in human liver cancer. Cancer Cell *13*, 153–166.

Yeung, M.L., Yasunaga, J., Bennasser, Y., Dusetti, N., Harris, D., Ahmad, N., Matsuoka, M., and Jeang, K.T. (2008). Roles for microRNAs, miR-93 and miR-130b, and tumor protein 53-induced nuclear protein 1 tumor suppressor in cell growth dysregulation by human T-cell lymphotrophic virus 1. Cancer Res. *68*, 8976–8985.

Yin, S., Li, J., Hu, C., Chen, X., Yao, M., Yan, M., Jiang, G., Ge, C., Xie, H., Wan, D., et al. (2007). CD133 positive hepatocellular carcinoma cells possess high capacity for tumorigenicity. Int. J. Cancer *120*, 1444–1450.

Yu, F., Yao, H., Zhu, P., Zhang, X., Pan, Q., Gong, C., Huang, Y., Hu, X., Su, F., Lieberman, J., and Song, E. (2007). let-7 regulates self renewal and tumorigenicity of breast cancer cells. Cell *131*, 1109–1123.

Zhu, Z., Hao, X., Yan, M., Yao, M., Ge, C., Gu, J., and Li, J. (2010). Cancer stem/progenitor cells are highly enriched in CD133+CD44+ population in hepatocellular carcinoma. Int. J. Cancer *126*, 2067–2078.